



Review

Titanium(IV) complexes as direct TiO₂ photosensitizers

Wojciech Macyk^{a,*}, Konrad Szaciłowski^{a,b}, Grażyna Stochel^a, Marta Buchalska^a,
Joanna Kuncewicz^a, Przemysław Łabuz^a

^a Wydział Chemii, Uniwersytet Jagielloński, ul. Ingardena 3, 30-060 Kraków, Poland

^b Akademia Górniczo-Hutnicza, Wydział Metali Nieżelaznych, al. Mickiewicza 30, 30-059 Kraków, Poland

Contents

1. Introduction	2688
2. Titanium(IV) surface complexes—structure	2688
2.1. Surface of titanium dioxide	2688
2.2. Monodentate complexes	2689
2.2.1. Alcohols	2689
2.2.2. Phenols	2689
2.3. Bidentate complexes	2689
2.3.1. Monocarboxylic aliphatic acids	2689
2.3.2. Dicarboxylic aliphatic acids	2689
2.3.3. Ascorbic acid	2690
2.3.4. Catechol	2690
2.3.5. Benzoic acid	2690
2.3.6. Phthalic acid	2690
2.3.7. Salicylic acid	2691
2.3.8. Gallic acid	2691
2.4. Polynuclear complexes	2691
3. Titanium(IV) surface complexes—electronic structure and photosensitization	2692
3.1. Electronic structure of neat titanium dioxide	2692
3.2. Quantum-mechanical description of molecule–semiconductor interactions	2692
3.3. Computational studies on surface Ti ^{IV} complexes	2694
4. Photoreactivity of titanium(IV) surface complexes	2697
4.1. Photoelectrochemistry	2697
4.2. Photocatalysis	2699
5. Potential applications and perspectives	2699
Acknowledgements	2700
References	2700

ARTICLE INFO

Article history:

Received 14 October 2009

Accepted 30 December 2009

Available online 7 January 2010

Keywords:

Titanium(IV) complexes

Titanium dioxide

Photocatalysis

Photoinduced electron transfer

Photosensitization

ABSTRACT

Titanium dioxide photosensitization may be achieved in various ways, involving surface modification with appropriate species. The photosensitization process requires a visible light-induced electron or hole injection into conduction or valence band, respectively. Efficiency of this process depends on electronic interaction between the photosensitizer moiety (surface complex) and TiO₂ particle. At least two types of the charge injection mechanisms may be distinguished—in the first, charge is transferred from the excited state of the sensitizer molecule to the conduction or valence band while the second mechanism involves a direct molecule-to-band charge transfer (MBCT). The MBCT process can be realized by surface titanium(IV) complexes with various organic and sometimes inorganic ligands. Catechol, phthalic acid or salicylic acid derivatives, as well as cyanometallate anions, upon chemisorption at TiO₂ surface constitute an especially interesting group of ligands to yield various titanium(IV) surface complexes. Geometry of these complexes, electronic structures and possibility of their use as photosensitizers of TiO₂ are discussed on the basis of experimental data and quantum-chemical modeling. Also prospective applications of photoinduced electron transfer and photocatalytic activity of such systems are presented.

© 2010 Elsevier B.V. All rights reserved.

* Corresponding author. Tel.: +48 12 6632005; fax: +48 12 6320515.

E-mail address: macyk@chemia.uj.edu.pl (W. Macyk).

1. Introduction

Modern photochemistry of coordination compounds seems to have left homogeneous solutions and now focuses on the photochemistry at interfaces [1]. Increasing efforts in constructing efficient solar cells or photocatalysts activated by solar or – even better – visible light, forced researchers to focus on photochemistry at surfaces of solids, particularly semiconductors. Adsorbed or chemisorbed transition metal complexes may alter the electronic structure (and hence spectroscopic and redox properties) of wide band gap semiconductors [2,3]. The surface modification of TiO_2 also influences quantum yields of photoinduced electron transfer processes. In particular, photosensitization of titanium dioxide gains a great attention since this material finds applications as a photoactive material in photovoltaics (dye sensitized solar cells; DSSC), optoelectronics (photoswitchable logic gates) and photocatalysis (water, air, surface detoxification and disinfection) [4–7].

Surface complexes playing the role of TiO_2 photosensitizers are usually constituted of a transition metal ion with inorganic or organic ligands. In the latter case the ligands are coordinatively bound to the central ion and covalently linked to the titanium dioxide surface via various anchors (e.g. hydroxyl, carboxyl, amino and other groups). Inorganic ligands (e.g. CN^- , F^- , PO_4^{3-}) can also play the role of bridges between surface titanium and metal centers. The photosensitization effect is based on the photoinduced electron injection from the surface complex to conduction band (CB) of the semiconducting support. Alternatively, a hole might be injected to the valence band (VB). Photoinduced charge injection can be realized as a so called *direct* or *indirect* photosensitization. These processes are based on optical electron transfer (OET) and photoinduced electron transfer (PET), respectively. In the former case the excited state of the photosensitizer can be described as an oxidized surface moiety and reduced titanium center since titanium(III) can be considered as a trapped electron in the conduction band of TiO_2 [8]. On the other hand, the indirect photosensitization is a multistep process involving generation of an excited state of the surface complex and consecutive charge transfer to the appropriate band of a semiconductor. The direct photosensitization should result in a more efficient electron transfer to the conduction band, however, the back electron transfer process might also be facile. Indirect photosensitization in general is characterized by a lower efficiency of the electron injection, but the back electron transfer is hindered due to an energy barrier. Further differences between these types of photosensitization will be discussed in next paragraphs of this paper.

A specific class of surface complexes formed at titanium dioxide comprises titanium(IV) complexes synthesized upon chemisorption of organic ligands onto titania. Similar moieties used as anchoring groups binding external complexes to the surface may be regarded themselves as ligands. Surface species of $[\equiv\text{Ti}-\text{L}]$ type can be easily formed. Ligand-to-metal charge transfer (LMCT) in this case is equivalent to the injection of electron to the conduction band—in both cases the Ti^{III} species is generated. Therefore in such situation the photoinduced charge transfer can be described as ligand-to-band charge transfer (LBCT) instead of LMCT. An effective photosensitization of titanium dioxide by such complexes can be achieved only under certain circumstances: (i) the energy of LBCT is lower than the band gap energy of TiO_2 (<3.2 eV) and (ii) absorption coefficient of the LBCT transition is high (allowed transition). However, the practical application of such materials is limited by efficiency of back electron transfer.

In this paper a brief description of various titanium(IV) complexes synthesized *in situ* at the surface of TiO_2 is given. Our goal is to show possible correlations between structures of Ti^{IV} complexes (mainly with O-ligands) and applicability for titanium dioxide pho-

tosensitization as well as to discuss possibility of application of these systems in photocatalysis, photovoltaics and optoelectronics.

2. Titanium(IV) surface complexes—structure

2.1. Surface of titanium dioxide

The crystal structure of the titanium dioxide surface strongly influences its surface chemistry and photoactivity. Every crystal plane is characterized by different amounts of various titanium and oxygen sites. Thus, the description of the adsorption processes and ligand coordination on a definite TiO_2 surface requires a definition of crystal face at which these processes take place. Detailed studies concerning adsorbate/metal oxide surface interactions always refer to a specific crystal plane. The most often characterized and studied TiO_2 crystal planes are the most stable (101) anatase [9–11] and (110) rutile [11–14] faces.

The density (given as number of $-\text{OH}$ groups per square nanometer) and acidity of surface hydroxyl groups are strongly affected by the coordination environment of the surface titanium(IV) ions [14,15]. The most common and simple representation of hydrated surface, which can also be used in rationalization of surface chemistry, is a multisite surface complexation [16,17]. In this model, the surface of TiO_2 is described as an array of Ti^{IV} and $\text{O}^{\text{II-}}$ sites. Upon dissociative chemisorption of water onto crystal faces of titanium dioxide three types of titanium(IV) sites, sometimes denoted as 'A', 'B' and 'C', are formed (Fig. 1). The 'A' sites are constituted of hexacoordinated surface titanium atoms with five bridging oxo anions (O^{2-}) and hydroxyl group (OH^-) as ligands. At 'B' sites O^{2-} bridges are protonated forming $>\text{OH}$ links between titanium centers [16,18,19]. Titanium with four oxo ligands forms 'C' sites at the edges and corners of crystals [15,19]. Remaining coordination sites can be occupied by other ligands (H_2O , OH^-). The 'C' sites show a strong Lewis acidity due to two available coordination sites.

All sites of titanium dioxide undergo surface protonation and deprotonation reactions, however, mainly sites with surface titanium ion are susceptible to surface complexation with external ligands [19]. The chemisorption of organic compounds occurring at the TiO_2 surface may be considered as a Lewis and/or Brønsted acid–base reaction [20]. Donor groups containing oxygen, nitrogen or sulfur atoms may act as a Lewis base and donate electrons to the Lewis acids (surface Ti^{IV}) [12]. The structure and stability of surface complexes of titanium(IV) are determined by type of TiO_2 crystal plane, accessibility of titanium ions, type of ligating sites of organic ligands, pH, etc. Three basic structures of simple surface complexes can be distinguished: (i) monodentate structure with the organic ligand occupying one coordination site of tita-

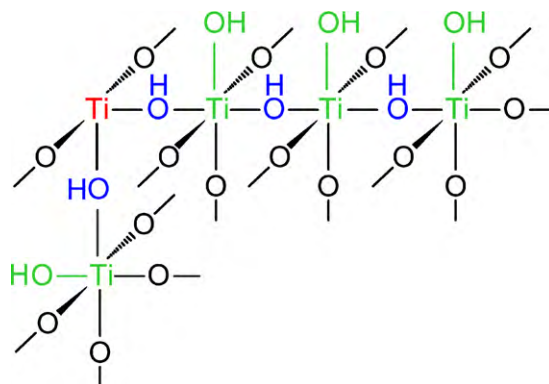


Fig. 1. Three types of Ti sites at titanium dioxide surface: 'A'—green, 'B'—blue, and 'C'—red.

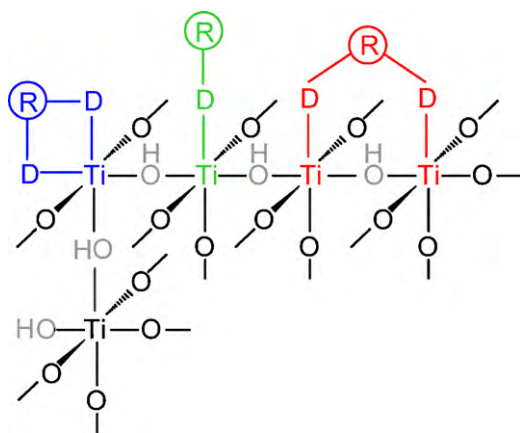


Fig. 2. Types of titanium(IV) surface complexes structures: monodentate—green, bidentate chelating—blue, and bidentate bridging—red.

nium; (ii) bidentate chelating structure with the ligand occupying two coordination sites; (iii) bidentate bridging structure composed of chelating ligand binding two neighboring Ti centers (Fig. 2) [21]. The first group comprises also polynuclear complexes with bridging ligands binding not the neighboring titanium ions but titanium and other metal ions. Not every surface Ti site is prone to be involved in each type of structure, for instance titanium centers bound with five oxo ligands can form monodentate or bridging structures while the formation of a bidentate chelating complex requires substitution of one oxo ligand. In the next paragraphs the structures of surface Ti complexes with various organic ligands (mainly O-donors) are presented.

2.2. Monodentate complexes

2.2.1. Alcohols

The interaction of aliphatic alcohols with titanium dioxide surface is broadly studied mainly because of its great influence on photocatalytic processes occurring in the presence of these molecules. Simple aliphatic alcohols, such as methanol, ethanol, 1- and 2-propanol undergo physical (molecular) and chemical adsorption through hydroxyl group at the titanium dioxide surface [22,23]. In the case of ethanol, the physical and chemical adsorption was confirmed by ^{13}C cross-polarization MAS NMR measurements [24,25]. ^{13}C -MAS experiments indicated dissociative chemisorption of ethanol leading to formation of multiple surface complexes [24]. It was proposed that ethoxide species are attached to the surface sites characterized by different electronic environments. Similarly the formation of different 2-propoxide species upon the dissociative adsorption of 2-propanol on TiO_2 surface at different sites was observed [26]. More detailed characterization of the adsorbed ethoxide species was performed basing on XPS (X-ray Photoelectron Spectroscopy) and TPD (Temperature Programmed Desorption) measurements [27]. Two different types of adsorbed ethoxy surface complexes were proposed: the ethoxy group bound to the surface Ti sites and ethoxy moiety attached to the surface “bridging oxygen” vacancy. Dissociative adsorption of simple aliphatic alcohols, however, does not influence significantly spectroscopic properties of complexed TiO_2 .

2.2.2. Phenols

Phenol as well as 4-chlorophenol has a moderate affinity to the TiO_2 surface [15,28]. Diffuse reflectance IR spectroscopy and FTIR measurements confirmed a very weak chemisorption of phenol at TiO_2 surface occurring with the formation of phenolate adsorbate [29,30]. The formed complexes are characterized by low stability constants. The observed weak chemisorption may be explained

by inability of phenol and 4-chlorophenol to form ring-structured surface complexes (*vide infra*—bidentate complexes).

2.3. Bidentate complexes

The formation of bidentate surface complexes is possible only if the ligand possesses at least two donor groups, or one group containing two donor atoms. The possibility of bidentate structures formation does not exclude monodentate complexation mode nor physisorption.

2.3.1. Monocarboxylic aliphatic acids

Carboxylic acids are well known for their complexation ability and therefore carboxyl groups are commonly used anchors chosen for covalent binding of any organic or inorganic molecules. Binding at ‘A’ and ‘C’ sites may lead to formation of titanium(IV) complexes [31]. The interaction of RCOOH with TiO_2 surface occurs often through the acid dissociation and exchange of surface hydroxyl groups with carboxylate anions (formation of RCOO-Ti bond).

Formic acid is often treated as a simple model molecule in experimental and theoretical studies of the RCOO-Ti bond formation. It undergoes a dissociative adsorption at the TiO_2 surface [9,12,32]. Several experimental studies [32] (FTIR, Raman spectroscopy) as well as theoretical calculations [9,12,32] (DFT) have shown that formate anion binds to titanium dioxide surface (rutile (0 1 1) and (1 1 0) planes and anatase (1 0 1) plane) creating mainly bidentate bridging complex, where each oxygen atom of $-\text{COO}^-$ group is attached to two adjacent surface Ti sites while dissociated proton is transferred to a surface oxygen site. A monodentate configuration is less favored mode—in this case one of the oxygen atoms is bound to a surface titanium site while the other is supposed to interact with a surface hydroxyl group (‘B’ site). The bidentate chelating coordination appears to be thermodynamically unstable.

Other aliphatic monocarboxylic acids, e.g. acetic acid [11,12,32] also show a tendency to dissociative adsorption onto the TiO_2 surface (rutile (0 1 1)) with formation of bidentate bridging complexes as the most stable configuration [11,32]. Chemisorption of formic, acetic and citric acids (tricarboxylic acid) was observed only in suspensions at pH providing at least partially hydroxylated surface ($\text{pH} < 7$).

2.3.2. Dicarboxylic aliphatic acids

Organic acids with adjacent carboxyl groups can interact with TiO_2 surface forming surface complexes that may be different from those favored in the case of monocarboxylic acids. In general dicarboxylic acids form more stable surface complexes as compared to monocarboxylic acids [17].

Oxalic acid is the simplest example of a dicarboxylic acid. This model compound undergoes a strong dissociative adsorption onto the TiO_2 surface [17,33]. Several studies (ATR-FTIR) have proven that strong inner-sphere surface complexes are generated [21,33,34]. Three different structures of these surface species were proposed: bidentate chelating [21,33–35] and/or bidentate bridging [20,21,33,36] where two oxygen atoms of each carboxyl group are attached to the same or adjacent Ti atoms while two remaining oxygen atoms are turned away from the surface (Fig. 3), and monodentate (protonated adsorbed oxalate and/or strongly hydrogen-bonded oxalate or protonated oxalate) which may appear at low pH [21,33–35,37]. The surface ring structures are considered as more favored which is in agreement with theoretical calculations proving that a bidentate bridging complex formed at the anatase surface is the most stable form of the adsorbed oxalic acid [20].

Other dicarboxylic aliphatic acids, malonic and succinic acids, adsorb in a different manner. Although surface complexes configurations for both compounds are not completely proven there is

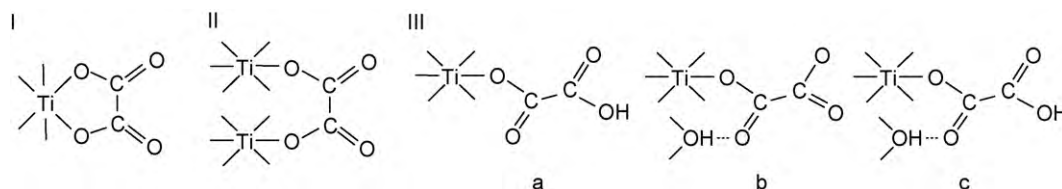


Fig. 3. Types of TiO_2 -oxalate surface complexes: bidentate chelating (I), bidentate bridging (II) and proposed monodentate structures (III): protonated adsorbed oxalate (a), strongly hydrogen-bonded oxalate (b) or protonated oxalate (c).

an evidence (ATR-FTIR) that structures of the adsorbed species of these two compounds do not involve $\text{C}=\text{O}$ bonds. It is proposed that malonate and succinate can form three different surface complexes: monodentate structures stabilized with hydrogen bonds, bidentate chelating structure (four-member ring) and bidentate bridging structure (five-member ring). Every bidentate structure involves both oxygen atoms of each carboxyl group [21].

2.3.3. Ascorbic acid

Ascorbic acid may also act as an electron-donating ligand. FTIR studies on adsorption of vitamin c on the nanosized titanium dioxide surface confirmed the formation of bidentate surface complexes [38,39]. In the case of nanosized TiO_2 surface having a certain amount of undercoordinated sites ("corner defects"; $\text{Ti}=\text{O}$) chelating structure of surface species is favored. The ascorbic acid binds to surface Ti sites through both hydroxyl groups of the five-membered ring.

2.3.4. Catechol

Benzene derivatives with hydroxyl or carboxyl groups form very stable chelates with TiO_2 surface. Usually the complex formation involves replacement of TiO_2 surface hydroxyl groups by deprotonated ligands [16,40].

Catechol, a diprotic weak acid ($\text{pK}_{a1}=9.2$; $\text{pK}_{a2}=13.0$), forms stable complexes with Ti^{IV} [16,18]. The interaction of catechol molecules with TiO_2 surface (surface Ti ions) resembles the interaction of catechol with Ti^{IV} in solution [16,41]. Catechol adsorbs dissociatively at the titanium dioxide surface through the deprotonated hydroxyl groups [41,42]. Results of the experimental studies (FTIR [43], ATR-FTIR [37,41], adsorption isotherm studies [16,41], UPS (UV photoemission spectroscopy), STM [13]) have proven formation of the ring-structured surface complexes. On the basis of IR measurements two types of possible surface species were proposed: bidentate chelating, and bidentate bridging structures [16,37] since IR spectra do not differentiate these structures [37,41,43]. However, STM measurements combined with theoretical calculations have proven that in the case of catechol adsorption onto a rutile (110) surface, bidentate bridging complexes predominate. This form seems to be favored because of a similar distance between catechol groups and adjacent surface Ti centers [16]. Moreover, it was demonstrated that at higher concentrations of catechol two kinds of packing of adsorbed molecules may be formed: one involving H-bound monodentate complexes (with partially dissociated catechols) and the second one consisting of a mixture of H-bound monodentate and bidentate structures. In both cases hydrogen bonds are formed between the hydroxyl group of one catechol molecule (partially dissociated) and oxygen of the neighboring catechol molecule determining the left/right tilted configuration of these structures (Fig. 4) [13]. The monodentate complexes, however, do not introduce additional electronic states into the band gap of titanium dioxide, as proposed for bidentate species. Another computational study focused on the interaction of catechol with anatase- TiO_2 nanoparticles has shown that dissociated catechol molecules may coordinate to the defect $\text{Ti}=\text{O}$ surface sites leading to formation of very stable bidentate chelat-

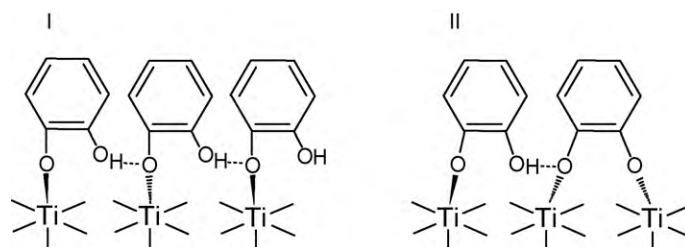


Fig. 4. Left/right tilted configuration of H-bound monodentate complexes with partially dissociated catechol ligands (I) and with a mixture of H-bound monodentate and bidentate structures (II).

ing surface complexes [10]. This type of defect occurs frequently at the surface of anatase nanoparticles. It was also proposed that bidentate chelating surface species are more favored than bidentate bridging complexes on (101) anatase plane. These results are in agreement with FTIR studies [39], confirming bidentate binding between ortho-hydroxyl groups and the TiO_2 surface.

2.3.5. Benzoic acid

Benzoic acid, compared to aliphatic carboxylic acids, adsorbs to a very little extent at the titanium dioxide surface (e.g. for anatase no adsorption [44] or a very weak adsorption [15] was reported basing on UV-vis spectroscopic measurements). CIR-FTIR (cylindrical internal reflection-FTIR) studies allowed to confirm the mechanism of dissociative adsorption of this molecule onto the anatase surface [44]. Results of these studies suggest that benzoic acid is attached to TiO_2 surface through two oxygen atoms of carboxyl group bound to one surface titanium(IV) ion (more likely) or two adjacent Ti centers. However, on the basis of STM, ESDIAD (electron stimulated desorption ion angular distribution) and LEED (low energy electron diffraction) measurements the bidentate bridging structure of the surface complexes (at the (110) plane) is more favored [45].

2.3.6. Phthalic acid

Phthalic acid strongly chemisorbs onto TiO_2 surface. Dissociative adsorption results in formation of stable ring complexes. Two different structures of these surface species are proposed: bidentate bridging where complexation of two Ti sites ('A' sites) occurs through two oxygen atoms of the same carboxyl group, and a more probably bidentate chelating structure with two oxygen atoms of both carboxyl groups attached to one surface Ti ion ('C' site; Fig. 5)

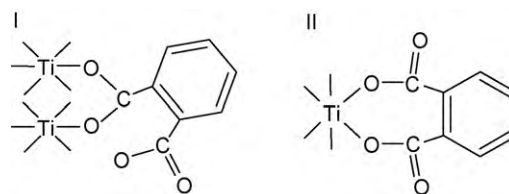


Fig. 5. Proposed structures of TiO_2 -phthalate complexes: bidentate bridging via one carboxyl group (I) and bidentate chelating involving two oxygen atoms from both carboxyl groups (II).

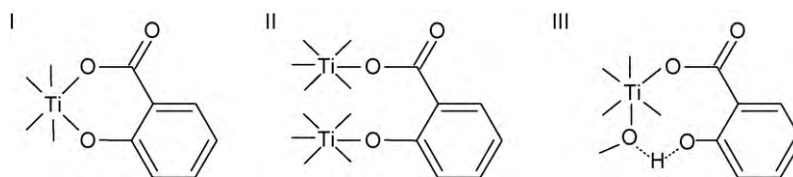


Fig. 6. Types of TiO_2 -salicylate complexes: bidentate chelating (I), bidentate bridging (II), and monodentate (III) structures.

[40,44]. Because of steric reasons other isomers of phthalic acid (*iso*- and *tere*-) bind to two adjacent Ti^{IV} surface sites 'A' forming bidentate bridging complexes. In the case of terephthalate (*p*-phthalic acid) complexation leads to a flat geometry in which the aromatic ring is parallel to the surface [40].

2.3.7. Salicylic acid

Salicylic acid, similarly to catechol, shows a great affinity to Ti^{IV} ions in solution and chemisorbs efficiently at the titanium dioxide surface. It adsorbs dissociatively forming a surface titanium complex involving both carboxyl and hydroxyl groups [17,34,44]. Two structures of the surface complexes are proposed: bidentate chelating [17,19,34,44] (structure I, Fig. 6) and less stable bidentate bridging, structure II, (or monodentate through the oxygen atom of carboxyl group, structure III) [19,34]. FTIR studies on the complexes formed at the surface of nanosized TiO_2 also confirmed presence of bidentate bonding [39]. In that case the bidentate chelating structure (structure I) is proposed. However, IR measurements are not sufficient to enable a complete distinction between these two surface ring structures, as in the case of oxalic acid or catechol.

2.3.8. Gallic acid

The ATF-FTIR studies proved that interaction between gallic acid (3,4,5-trihydroxybenzoic acid) and titanium dioxide surface leads to formation of inner-sphere ring surface complexes [41]. Gallic acid adsorbs at the TiO_2 surface through the complexation of two hydroxyl groups. In contrast to the salicylic acid, the carboxyl group is not involved in the surface complexation.

2.4. Polynuclear complexes

Various organometallic complexes of transition metals may be bound to the surface titanium centers through anchoring groups. As described above carboxyl groups can play the role of anchors. In this way a polynuclear complex is formed with bridging ligands capable of coordination to both Ti^{IV} and other metal ions (for instance Ru^{II} [4,5,46,47], Pt^{II} [48], Os^{II} [47,49], etc.). These structures, however, offer relatively long bridges between two metal ions constituted of many bonds. Although several of these complexes photosensitize TiO_2 effectively, as in the case of Ti-LL-Ru moieties used in dye sensitized solar cells, the electron photoinjection to the conduction band is a multistep process—generation of the excited state of the complex (usually MLCT excitation) is followed by the electron transfer to the conduction band. A similar situation takes place for Ti-O-Pt structures formed upon $[\text{PtCl}_6]^{2-}$ chemisorption at the titanium dioxide surface [50–53]. Although the bridging ligand is small the electron injection to the conduction band comprises two consecutive steps, i.e. LMCT excitation within platinum(IV) moiety and electron transfer. The mechanism of indirect photosensitization (electron injection to the conduction band of TiO_2 or electron transfer to Ti^{IV} from the excited state of photosensitizer) differs significantly from that of the direct one observed for simple surface complexes of titanium(IV) in which ligand-to-titanium charge transfer plays a predominant role [8]. Since titanium complexes participating in the direct photosensitization

are in the scope of this paper the other structures will not be described in detail.

A nice example of a polynuclear surface complex constituted of titanium(IV) and another metal ion participating in the direct sensitization of titanium dioxide is formed upon adsorption of hexa- or pentacyanoferrates(II) onto TiO_2 surface. In the case of $[\text{Fe}(\text{CN})_6]^{4-}$ complex [54] and $[\text{Fe}(\text{CN})_5\text{L}]^{3-}$ ($\text{L} = \text{NH}_3$, H_2O , thiodiethanol, thiodipropanol, dimethyl sulfoxide, etc.) [55,56] formation of $\text{Ti-N}\equiv\text{C-Fe}$ bridges takes place (Fig. 7). The reaction of hexa- and pentacyanoferrates with the surface of titanium dioxide crystals can be regarded as a nucleophilic substitution reaction with titanium ions playing the role of central ions and cyanoferrate anions acting as ligands. The formed binuclear complexes are characterized by a broad MMCT absorption band in the visible range that can be described as MBCT (molecule-to-band charge transfer) when titanium(IV) ion belongs to the TiO_2 matrix [55]. The same absorption bands are observed upon mixing aqueous solutions of pentacyanoferrates with colloidal solutions of titanium dioxide nanocrystals. In both cases the MMCT bands are broad and extend to 600–650 nm, except for the dimethyl sulfoxide complex, which exhibits only a very weak sensitization towards visible light. The most probable mode of $[\text{Fe}(\text{CN})_5\text{L}]^{3-}$ binding is that via the axial cyanide ligand, as demonstrated by quantum-chemical calculations [55]. This mode is predominant especially in the case of a bulky sixth ligand [56].

Interesting systems were described by Yang et al. [57]. The authors studied photosensitization of titanium dioxide by chemisorbed $[\text{Fe}(\text{LL})(\text{CN})_4]^{2-}$ complexes, where LL = bpy (2,2'-bipyridine), dmb (4,4'-dimethyl-2,2'-bipyridine), or dpb (4,4'-diphenyl-2,2'-bipyridine). Electronic spectra of formed surface $[\text{Ti}]\text{-NC-Fe}(\text{LL})(\text{CN})_4$ species show both MLCT and MBCT (described also as MPCT, metal-to-particle charge transfer) bands. Either MLCT or MBCT excitation results in the electron injection to the conduction band of TiO_2 . The quantum yield for the MLCT process was environment dependent. The described surface modification constitutes a good example of system with competing direct and indirect photosensitization modes.

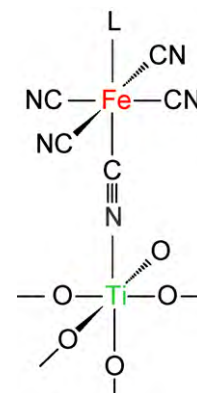


Fig. 7. Binuclear complex of pentacyanoferrate(II) with titanium(IV) formed upon chemisorption of a corresponding ferrate anion onto the surface of TiO_2 .

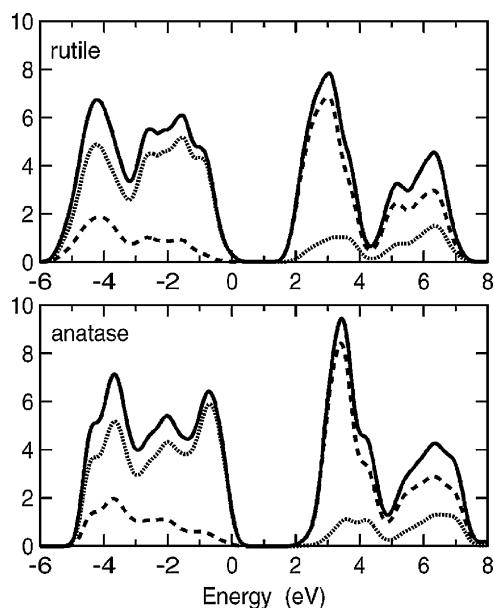


Fig. 8. Density of states for rutile and anatase modification of TiO_2 as calculated using DFT method [58]. Dashed and dotted lines represent partial density of states for titanium 3d and oxygen 2p orbitals, respectively. Reproduced from Ref. [58] with permission. Copyright American Chemical Society 2003.

3. Titanium(IV) surface complexes—electronic structure and photosensitization

3.1. Electronic structure of neat titanium dioxide

The total and partial densities of states of anatase and rutile polymorphs of titanium dioxide are shown in Fig. 8. The main contribution to the valence band involves oxygen 2p states that are bound to titanium 3d orbitals. The conduction band consists of titanium 3d orbitals which are involved in an antibonding interaction with oxygen 2p orbitals [58].

The upper valence bands can be decomposed into three main regions: the σ bonding in the lower energy region mainly due to oxygen p_σ bonding; the π bonding in the middle energy region; and oxygen p_π states in the higher energy region due to oxygen p_π nonbonding states at the top of the valence bands where the hybridization with d states is almost negligible. The contribution of the π bonding is much weaker than that of the σ bonding. The conduction bands are decomposed into titanium e_g (>5 eV) and t_{2g} bands (<5 eV). The d_{xy} states are dominantly located at the bottom

of the conduction bands [59]. This electronic structure renders titanium dioxide especially suitable for photoinduced electron transfer studies and with appropriate ligands may form complexes with strong electronic coupling. Other wide band gap semiconductors of similar band gap and band edge potentials show very different band structures (e.g. ZnO and SnO_2). While the conduction band of TiO_2 is comprised mainly from empty d orbitals of Ti^{4+} ions, the conduction bands of other similar semiconductors are comprised of empty s and p orbitals of Zn^{2+} and Sn^{4+} ions. Comparing these types of bands, d bands are typically narrower and have densities of states that are orders of magnitude higher than sp bands [60]. Furthermore, the lower part of the conduction band in TiO_2 consists of d orbitals of t_{2g} symmetry, which is assumed to allow stronger electronic coupling with the electron-donating moieties [61].

The contribution of oxygen 2p orbitals to the conduction band and titanium 3d orbitals to the valence band indicates strong interactions between Ti and O atoms and is a clear evidence of a strong covalent bonding between titanium and oxygen atoms. As a result, the excitation across the band gap involves both the O 2p and Ti 3d states [62].

3.2. Quantum-mechanical description of molecule–semiconductor interactions

Adsorption of molecular species onto semiconducting surfaces brings about perturbation of electronic structures of both counterparts [63]. This interaction usually consists in formation of coordination compounds involving surface (coordinatively unsaturated) titanium ions. On the other hand these interactions resemble formation of molecular electronic junctions, as molecular species are reacting with much larger (semi)conducting surfaces with well defined band structure (*vide supra*) [64–66]. Therefore these systems can be successfully described by two different formalisms: as molecular junctions following the Galperin–Nitzan model [67–70] or a semi-classical electron-transfer formalism. In the latter case two diverse approaches can be applied depending on the nature of electronic coupling. Strongly coupled systems are usually described by the Creutz–Brunschwig–Sutin model, [71–74] while for weakly coupled systems the Sakata–Hiramoto–Hashimoto model is more appropriate (*vide infra*) [75,76].

In the case of a weak electronic coupling between semiconductor band and surface molecule the photoinduced electron transfer should be considered as the only way of photosensitization. Details of the PET process depend on the conductivity type. In the case of n -type semiconductors electrons are injected to the conduction band (Fig. 9a) with possible contribution of the empty surface states. If the HOMO of the photosensitizer has sufficiently low energy, in the

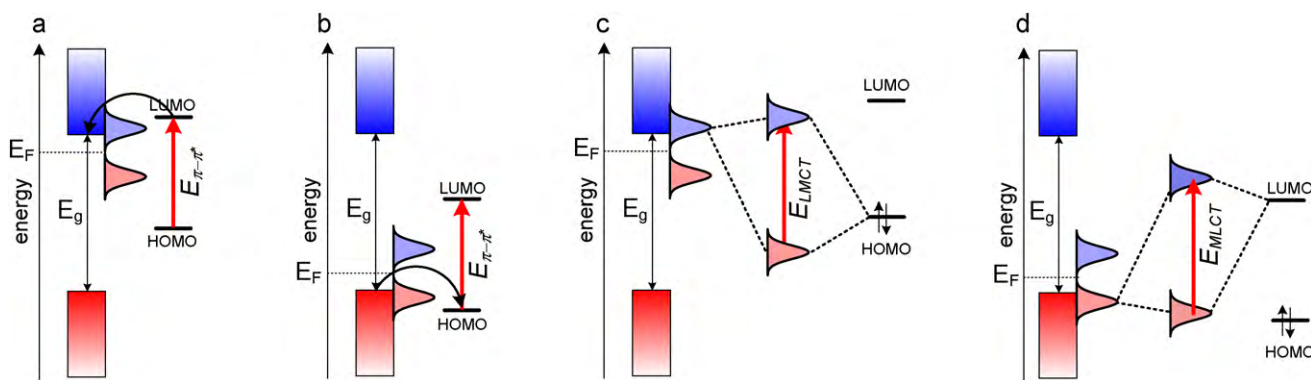


Fig. 9. Energy diagrams showing indirect photosensitization of n - (a) and p -type (b) semiconductors according to Sakata–Hiramoto–Hashimoto mechanism and direct photosensitization of n - (c) and p -type (d) semiconductors according to Creutz–Brunschwig–Sutin mechanism. Pale blue and pale red bell-shaped envelopes depict empty and occupied surface states, respectively. LMCT stands for ligand-to-metal charge transfer. MLCT—metal-to-ligand charge transfer, E_g —the band gap energy and E_F —the Fermi energy.

case of *p*-type semiconductor the hole injection into the valence band can be observed (Fig. 9b).

In the case of a strong electronic coupling the interaction of a ligand with the surface of the semiconductor leads to formation of surface coordination species (Fig. 9c and d). With a proper arrangement of molecular orbitals new energy levels are formed. In the case of *n*-type semiconductor (Fig. 9c) a bonding orbital is formed via interaction of the HOMO level of the surface ligand with the empty surface state. Resulting surface states with HOMO and LUMO character are mostly located at the surface ligand (electron donor) and belong to the conduction band, respectively. In this case excitation of the surface complex leads to optical electron transfer from the surface molecule to the conduction band. The opposite situation is observed in the case of the *p*-type semiconductor interaction with an electron acceptor (Fig. 9d).

According to the electronegativity difference between the reacting species, the chemical interaction occurs either between the HOMO (valence band or corresponding occupied surface state) of the semiconductor and the LUMO of the adsorbate (nucleophilic attack) or between LUMO (conduction band or corresponding empty surface state) of the semiconductor and HOMO of the adsorbate (electrophilic attack) [77]. The former case is usually observed in the case of *p*-type semiconductors interacting with electron acceptors, while the latter one in the case of *n*-type semiconductors and electron donors (Fig. 9). The detailed mechanism of photosensitization (direct electron transfer vs. excited state electron injection) is a consequence of the degree of electronic coupling between molecular orbitals of the adsorbate and energy levels within the appropriate bands (Fig. 10).

In contrast to physisorption (Fig. 10a) chemisorption always involves mutual interaction between the adsorbate and the substrate. A straightforward description is given by the Newns–Anderson model [78]. In this model a single electronic level $|a\rangle$ of the adsorbate is projected onto a continuum of Bloch states $|k\rangle$ constituting a band. In the absence of external stimuli only the electron transfer coupling is responsible for the broadening of molecular resonance [79]. If the surface–adsorbate interaction is smaller than the width of the band the distribution of the mixed states is described by a Lorentzian envelope of width expressed as Eq. (1):

$$\Gamma(E) = \pi \sum_k |V_{ET}(k)|^2 \delta(E - \varepsilon_k) \quad (1)$$

i.e. the $|a\rangle$ level is broadened into a resonance peak centered at ε_a [79].

Weak electronic coupling (Fig. 10a and b) favors the excited state electron injection, while strong electronic coupling (Fig. 10c) enforces the direct electron transfer mechanism, as it provides the framework for delocalized molecular orbitals encompassing both the adsorbate and some part of semiconductor's band. These two modes of photosensitization can be also understood as a competition between different components of a general Hamiltonian describing the molecule–semiconductor systems in the presence of radiation field.

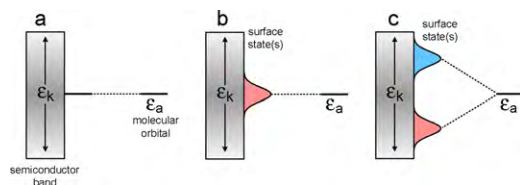


Fig. 10. Energy diagrams for surface-modified semiconductors in the case of physisorption with no electronic coupling (a); chemisorption with weak electronic coupling (b) and chemisorption with strong electronic coupling (c). ε_k stands for an electronic continuum of the metal or semiconductor electronic band.

The general Hamiltonian of this system (\hat{H}) can be defined as a sum of Hamiltonians for all components (\hat{H}_M , \hat{H}_S , and \hat{H}_R for molecule, semiconducting substrate and radiation field, respectively) and a coupling operator \hat{W} including all the physical processes within the system as formulated below Eqs. (2) and (3):

$$\hat{H} = \hat{H}_M + \hat{H}_S + \hat{H}_R + \hat{W} \quad (2)$$

$$\hat{W} = \hat{W}_{ET} + \hat{W}_{DC} + \hat{W}_{RM} + \hat{W}_{RS} + \hat{W}_{RMS} \quad (3)$$

This sum includes terms describing the following processes: electron transfer coupling between each isolated molecular electronic state of the surface moiety and the electronic continuum of the semiconductor (\hat{W}_{ET}); dipole-induced dipole coupling (energy transfer), which describes an interaction of the excited molecule and the dielectric response of the support (\hat{W}_{DC}); molecule–radiation field coupling describing light absorption by the isolated molecule (\hat{W}_{RM}); semiconductor–radiation field coupling depicting electronic excitations within semiconductor (\hat{W}_{RS}); and molecule–semiconductor–radiation field coupling, which describes a direct electronic transition between the semiconductor electronic continuum and a molecular electronic state or *vice versa* (\hat{W}_{RMS}). The process of semiconductor photosensitization by chemisorbed organic dyes or transition metal complexes can be in most cases described by a combination of \hat{W}_{RM} and \hat{W}_{ET} terms since the photosensitization involves light absorption by the chromophore and a consecutive electron transfer from the excited state of the molecule into the conduction band of the semiconductor. This type of photosensitization (indirect) differs from the direct photosensitization proceeding as an optical electron transfer from the surface-bound molecule directly to the semiconductor. The direct photosensitization, described by the \hat{W}_{RMS} term, was reported only for cyanoferrates [55–57,80–85], catechol [86–88] and ascorbic acid [38] modified titanium dioxide.

Indirect processes involve excitation of the surface dye followed by a rapid electron transfer from the excited state of the dye to the conduction band of the semiconductor. This process is favored in the case of covalently bound photosensitizers providing only a weak electronic coupling of the chromophore with bands or surface states of the semiconductor. Surface modifications based on various organic chromophores and metal complexes chemisorbed onto titanium dioxide and other wide band gap semiconductors surface photosensitize them according to the Sakata–Hashimoto–Hiramoto process (Fig. 9a and b) [75,76]. This process is fundamental for photosensitized solar cells, as a weak electronic coupling ensures high electron injection rates and low rates of back electron transfer.

Direct processes include also valence-to-conduction band excitations (i.e. fundamental transitions, \hat{W}_{RS}), photosensitization via bulk doping (substrate–radiation field coupling depicting optical properties of the semiconductor) and photophysical processes involving the molecule–substrate–radiation field coupling (\hat{W}_{RMS}). Interactions between semiconductor surfaces and molecular species modify the electronic properties of semiconductors, and alter spectroscopic and electrochemical properties of molecules bound to the semiconductor surfaces according to the level of electronic coupling (\hat{W}_{ET}) as depicted in Fig. 10. While a weak electronic coupling results in formation of surface state with Lorentzian distribution electronic state (Fig. 10b), in the case of a strong electronic coupling splitting of a single molecular level into two different surface states is observed (Fig. 10c). These states have the character of bonding and antibonding molecular orbitals, but may extend deeply into semiconductor and are usually involved in new allowed electronic transitions: molecule-to-band charge transfer (Fig. 9c) and band-to-molecule charge transfer (Fig. 9d). From the point of view of the semiconductor, these processes can be regarded as electron or hole injections, respectively. They result from a direct

optical electron transfer from the HOMO orbitals of the surface complexes to the conduction band or from the valence band to the LUMO orbitals of the surface electron acceptor, as predicted in theoretical models of Creutz et al. [71–73]. All these processes are responsible for a photoelectrochemical and photocatalytic activity of surface-modified TiO₂ upon visible light irradiation.

The indirect photosensitization based on PET has attracted most of attention as this process is crucial for dye sensitized solar cells. On the other hand these systems can be hardly regarded as based on titanium complexes. Organic photosensitizers or ruthenium complexes bound usually via carboxylate anchors inject electrons (or holes) from their electronic excited states. Here we concentrate on the systems based on a strong electronic interaction between titanium centers and adsorbed ligands enabling optical electron transfer (direct photosensitization mechanism).

3.3. Computational studies on surface Ti^{IV} complexes

Two systems have been characterized using advanced quantum-chemistry methods: TiO₂–hexacyanoferrate [54] and TiO₂–catechol [89]. The hexacyanoferrate@TiO₂ system was studied for a Ti₄₀O₈₀ cluster. The bonding of hexacyanoferrate via terminal nitrogen atom yields a system which locally can be regarded as a binuclear cyano-bridged complex. Electronic structure obtained at the B3LYP/6-311g*/3-21g* (ONIOM type calculation) revealed significant electronic coupling between iron(II) and titanium(IV) centers. The HOMO of the system is localized exclusively on iron complex with some contribution of the bridging ligand, while LUMO comprises of *d* orbitals of several titanium ions. The HOMO → LUMO transition is allowed and its energy is much lower (1.72 eV) than computed band gap of the Ti₄₀O₈₀ cluster (3.20 eV). These calculations confirm experimental evidence of the direct electron transfer from Fe^{II} to Ti^{IV} upon excitation.

The same conclusion was reached in the case of catecholate@TiO₂. Periodic DFT calculations revealed that the HOMO is localized almost exclusively on organic ligand (with only small contribution of neighboring titanium ions), while the LUMO is delocalized over all the titanium centers. Calculated PDOS (partial densities of state) spectra indicate, however, contribution of catecholate molecular orbitals in both valence and conduction band. Such arrangement is rather disfavoring the application of such systems in photovoltaics and photocatalysis. Spatial overlap of electron donor (catecholate) and electron acceptor (TiO₂ conduction band) orbitals may facilitate electron-hole recombination thus decreasing the photogenerated charge carrier quantum yield. The same conclusions were met in quantum-chemical study of dopamine chemisorbed onto small titanium dioxide clusters [90] and semiempirical study of TiO₂–anthocyanine [91] and TiO₂–catechol [10] systems.

DFT calculations for large systems require a large computational power, so very simple models of TiO₂–photosensitizer were successfully tested [55,85,92,93]. The simplified diagnostic method is based on simple titanium complexes containing [Ti(OH)₂]²⁺ moiety bound to the organic ligand or other metal center. These diagnostic tools have confirmed the degree of electronic coupling between titanium centers and chemisorbed molecules as a function of binding mode and electronic properties of the adsorbate.

The next step in computational analysis of these interactions should involve estimation of thermodynamic factors governing metal–ligand interactions, i.e. global Mulliken electronegativity and hardness (softness) of the ligands and metal centers.

Density functional theory assumes that the electronegativity χ is the negative derivative of the total energy E of an atom or molecule in the ground state with respect to number of electrons

N at a constant external potential v :

$$\chi = -\left(\frac{\partial E}{\partial N}\right)_v = -\mu \quad (4)$$

Mulliken electronegativity is a negative value of chemical potential of an electron in the system. Furthermore, the chemical reactivity of a molecule can be estimated from global hardness η (or softness S):

$$\eta = -\left(\frac{\partial \mu}{\partial N}\right)_v = \frac{1}{S} \quad (5)$$

Both Mulliken electronegativity and global hardness can be extracted from DFT results using Koopmans–Janak approximation [94,95]:

$$\chi = \frac{E_{\text{LUMO}} + E_{\text{HOMO}}}{2} \quad (6)$$

$$\mu = \frac{E_{\text{LUMO}} - E_{\text{HOMO}}}{2} \quad (7)$$

For semiconducting materials the Mulliken electronegativity can be understood as a position of the Fermi level relative to the vacuum level and global hardness of the semiconducting surface is equal to half of the surface forbidden gap. This yields the Mulliken electronegativity of anatase equal 4.3 eV [96] and the global hardness of 1.6 eV [97].

Modeling of larger systems should also involve localized equivalent of electronegativity, i.e. the Fukui function:

$$f(\vec{r}) = \left(\frac{\partial \rho(\vec{r})}{\partial N}\right)_v \quad (9)$$

which defines the response of the electron density $\rho(\vec{r})$ of the molecular system to the change of the number of electrons at constant external potential. In turn local softness defined as follows:


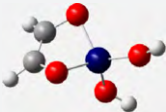
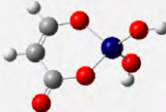
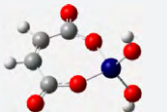
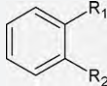
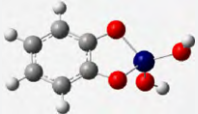
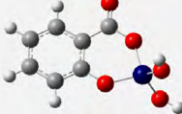
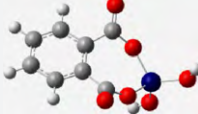
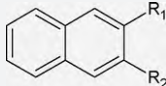
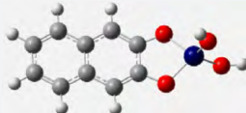
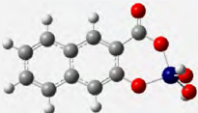
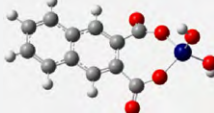
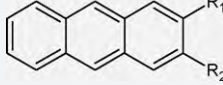
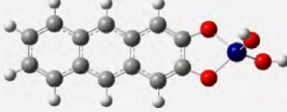
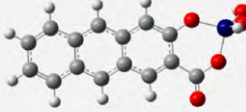
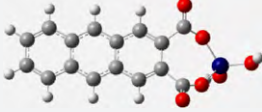
$$s(\vec{r}) = \left(\frac{\partial \rho(\vec{r})}{\partial \mu}\right)_v \quad (10)$$

determines the response of the electron density of the system to the change in chemical potential at the constant external potential (i.e. electric field generated by nuclei) [77]. While the localized indices $f(\vec{r})$ and $s(\vec{r})$ provide information on local reactivity of semiconducting surface with specific molecules, the global indices can be a useful compromise between computational expenses and predictive efficiency.

A series of model titanium complexes of [TiL(OH)₂] type complexes were designed and optimized at the B3PW91/DGDZVP level of theory. Three simple ligands (catecholate, salicylate and phthalate) were modified via extension of the aromatic ring system to naphthalene and anthracene derivatives (Table 1). Also enediol-type ligands, mimicking the fragment of ascorbic acid, were included in this series. Preliminary analysis shows that all the studied complexes are stable and the geometry of the complex depends only on the donating groups, while the aromatic moiety has no effects on the structures of model complexes.

The affinity of the deprotonated ligands towards the TiO₂ surface was probed via determination of Mulliken electronegativities and global hardness and softness of the deprotonated ligands. The data are collected in Table 2. The anchoring group configuration (two hydroxyls, two carboxyls or a combination of both) strongly influences the Mulliken electronegativity, while global hardness only slightly increases with increasing number of carboxylates. This results from a much higher accessibility of oxygen lone electron pairs for formation of coordination bond of carboxylates as compared with phenolates. The χ and S indices, in turn, strongly

Table 1Optimized geometries for various $[\text{TiL}(\text{OH})_2]$ model complexes at the B3PW91/DGDZVP level of theory.

Ligand framework	$\text{R}_1 = \text{OH}$ $\text{R}_2 = \text{OH}$	$\text{R}_1 = \text{OH}$ $\text{R}_2 = \text{COOH}$	$\text{R}_1 = \text{COOH}$ $\text{R}_2 = \text{COOH}$
			
			
			
			

correlate with the size of the π -electron systems: softness significantly increases with increasing aromatic system. It is quite natural, as with enlargement of delocalized π orbitals the polarizability of the molecule increases. Photosensitizers based on naphthyl skeleton seem to be best suited for titanium dioxide surface due to the best matching of both Mulliken electronegativities and hardness.

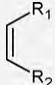
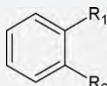
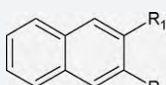
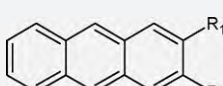
The above analysis, however, cannot give any valuable predictions regarding the nature and reactivity of the semiconductor–photosensitizer system in the excited state. The simplest tool to address this issue is the analysis of frontier orbital contours and charge transfer transitions. In all the studied systems the HOMO orbitals are localized mainly at the organic ligand and only a small fraction of HOMO is localized at titanium centers (Table 3). This qualitative observation is further supported with Mulliken population analysis of model complexes (Table 4) [98]. LUMO is localized mainly at titanium centers and the contribution of the ligand in LUMO decreases when carboxylate anchors are applied. Apparent increase of ligand contribution in LUMO in the

case of dicarboxylate ligands results from high contribution of oxygen atoms (up to 8%), while the aromatic part of the ligand does not significantly contribute to LUMO. This analysis indicates, that carboxylate anchors may yield slightly less efficient photosensitization, but due to a much weaker spatial mixing of HOMO and LUMO the recombination processes should be much less probable. Significant exception of this scheme is presented by simple ethene-derived ligands. They exhibit much stronger delocalization of HOMO and LUMO over the whole complex molecule.

Small, single-ring aromatic systems cannot provide a significant spatial isolation of HOMO and LUMO orbitals, which in turn may lead to extensive excited state deactivation. Extension of the aromatic system (with all anchoring configurations) results in effective isolation of HOMOs and LUMOs which in turn disturbs configurational mixing and thus stabilizes charge transfer excited state. The same stabilization can be observed on modification of the binding mode. While binding via two hydroxyls provides a platform for efficient delocalization of π orbitals into semiconductor conduc-

Table 2

Thermodynamic indices of various ligands (in the form of dianions) calculated from DFT data obtained at the B3PW91/DGDZVP level of theory.


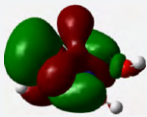
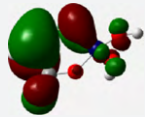
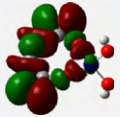
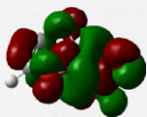
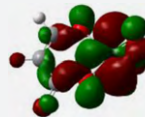
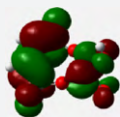
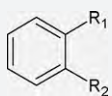
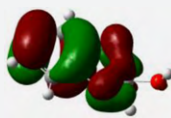
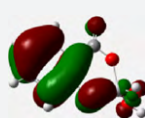
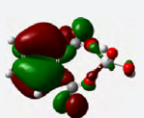
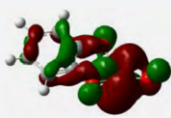
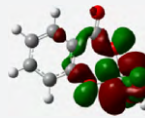
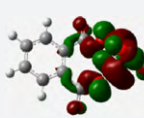
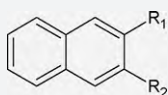
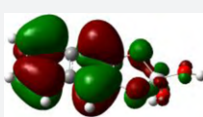
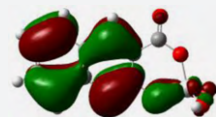
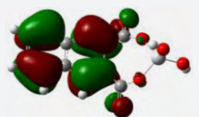
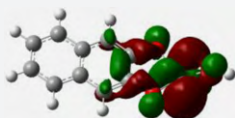
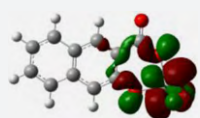
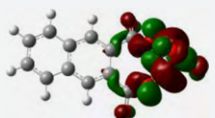
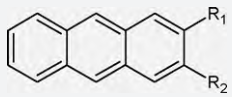

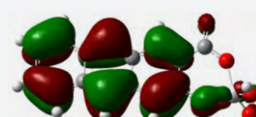
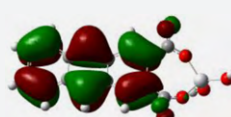
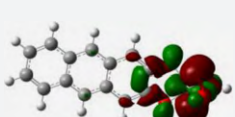
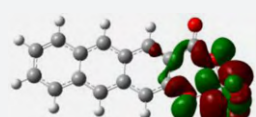
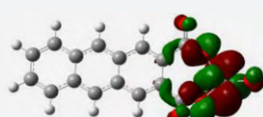
Ligand framework	Donor groups	χ/eV^a	η/eV^b	$S/\text{eV}^{-1}{}^c$
	$\text{R}_1 = \text{OH}, \text{R}_2 = \text{OH}$	11.24	3.29	0.30
	$\text{R}_1 = \text{OH}, \text{R}_2 = \text{COOH}$	7.37	2.86	0.35
	$\text{R}_1 = \text{COOH}, \text{R}_2 = \text{COOH}$	5.35	2.68	0.37
	$\text{R}_1 = \text{OH}, \text{R}_2 = \text{OH}$	7.70	2.29	0.44
	$\text{R}_1 = \text{OH}, \text{R}_2 = \text{COOH}$	5.84	2.27	0.44
	$\text{R}_1 = \text{COOH}, \text{R}_2 = \text{COOH}$	4.44	2.29	0.44
	$\text{R}_1 = \text{OH}, \text{R}_2 = \text{OH}$	5.59	1.73	0.58
	$\text{R}_1 = \text{OH}, \text{R}_2 = \text{COOH}$	4.27	1.71	0.58
	$\text{R}_1 = \text{COOH}, \text{R}_2 = \text{COOH}$	3.21	1.58	0.63
	$\text{R}_1 = \text{OH}, \text{R}_2 = \text{OH}$	4.22	1.33	0.75
	$\text{R}_1 = \text{OH}, \text{R}_2 = \text{COOH}$	3.8	1.28	0.78
	$\text{R}_1 = \text{COOH}, \text{R}_2 = \text{COOH}$	2.31	1.12	0.90

^a Mulliken electronegativity calculated according to Koopmans–Janak approximation (cf. Eq. (6)).

^b Ligand hardness calculated according to Koopmans–Janak approximation (cf. Eq. (7)).

^c Ligand softness (cf. Eq. (5)).

Table 3Contours of HOMO and LUMO orbitals for various $[\text{TiL}(\text{OH})_2]$ model complexes as calculated on the B3PW91/DGDZVP level of theory.

Ligand framework	Orbital	$\text{R}_1 = \text{OH}$ $\text{R}_2 = \text{OH}$	$\text{R}_1 = \text{OH}$ $\text{R}_2 = \text{COOH}$	$\text{R}_1 = \text{COOH}$ $\text{R}_2 = \text{COOH}$
	HOMO			
	LUMO			
	HOMO			
	LUMO			
	HOMO			
	LUMO			
	HOMO			
	LUMO			

tion band, application of carboxylate anchor provides more efficient decoupling of ground and excited states.

Excited state energies obtained from TD-DFT method also strongly correlate with both the structure of the aromatic part of the photosensitizer and the binding mode (Table 5). Enlarging π -electron framework results in decrease of the energy of $\text{HOMO} \rightarrow \text{LUMO}$ transition of charge transfer character, i.e. lower energy is needed to inject an electron into the conduction band of TiO_2 . The binding mode also affects this energy: the energy of the first singlet state increases for all the aromatic ligands in the series:



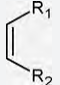
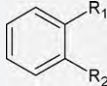
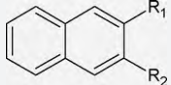
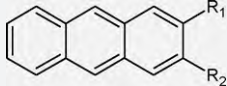
This is related not only to the efficiency of ligand-titanium orbital overlap, but also electrostatic factor associated with electron transfer must be taken into account. Two oxygen atoms in each carboxylate ligand generate an electrostatic energy barrier much higher than in the case of phenolate-type bonding. The only ligands which do not follow this trend are the ethene-derived ligands. This results from a very strong delocalization of molecular orbitals over the whole molecule. The relative differences in calculated energies of $\text{HOMO} \rightarrow \text{LUMO}$ transitions are in good agreement with

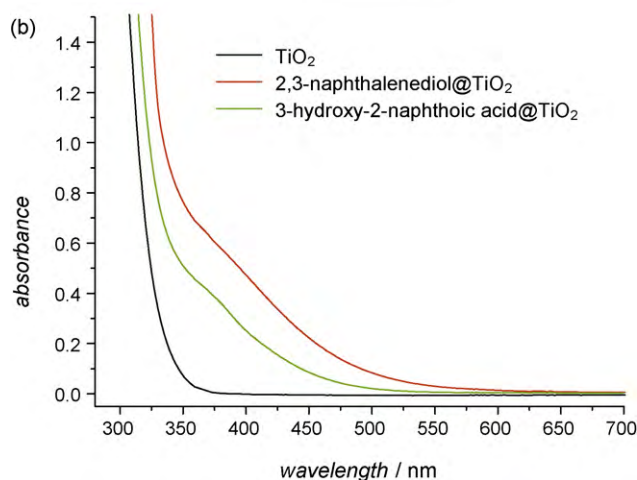
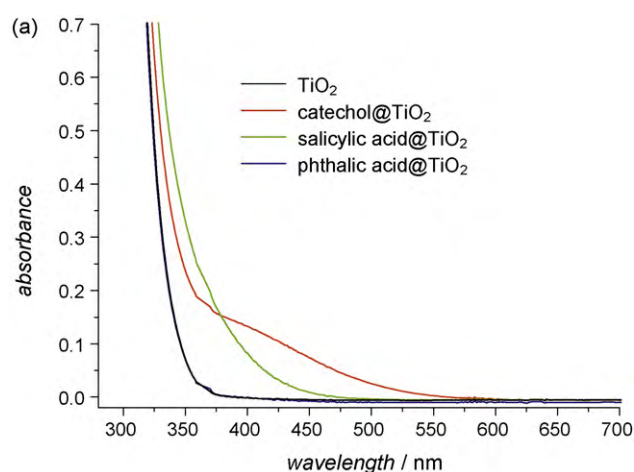
recorded spectra of titanium dioxide nanoparticles modified with appropriate ligands (Fig. 11)—the transition energy increases with decreasing size of the π -electron framework and increasing number of carboxyl groups.

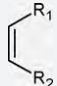
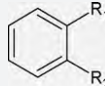
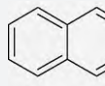
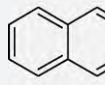
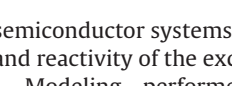
The lowest LMCT transition energy correlates also with Mulliken electronegativity and global hardness of the ligand (Fig. 12). In the case of all aromatic ligands, an increase of Mulliken electronegativity of the ligand results in a decrease of the S_1 energy. The same effect is observed in the case of decreasing hardness (increasing softness) of the ligand. This observation is consistent with metal–ligand interaction from the point of view of hard and soft acids and bases theory. Decrease in electronic coupling between the chemisorbed ligand and the titanium centers within the TiO_2 crystal results in indirect photosensitization via electron injection from locally excited surface molecule. These processes are usually observed with molecules that contain electron-withdrawing substituents, like quinone moiety, halogen atoms, etc. [93,99,100].

Thus, simple quantum-chemical modeling of photosensitization processes using simplified mononuclear models can be used as a diagnostic tool to estimate both the stability of photosensitizer-

Table 4Composition (%) of HOMO and LUMO orbitals for various [TiL(OH)₂] model complexes as calculated on the B3PW91/DGDZVP level of theory with tight convergence criteria.

Ligand	Orbital	R ₁ = OH R ₂ = OH		R ₁ = OH R ₂ = COOH		R ₁ = COOH R ₂ = COOH	
		Ti(OH) ₂	L	Ti(OH) ₂	L	Ti(OH) ₂	L
	HOMO	19.48	80.52	4.33	95.67	1.38	98.61
	LUMO	85.93	14.07	88.09	11.91	39.91	60.09
	HOMO	8.24	91.96	4.85	95.15	0.90	99.10
	LUMO	87.85	12.15	88.92	11.08	86.79	13.21
	HOMO	2.49	97.51	2.90	97.10	0.14	99.86
	LUMO	88.62	11.38	89.09	10.91	83.70	16.30
	HOMO	2.38	97.62	1.98	98.02	0.20	99.80
	LUMO	89.04	10.96	89.80	10.20	86.47	13.53

**Fig. 11.** Absorption spectra of TiO₂ nanoparticles with chemisorbed catechol, salicylic acid, phthalic acid (a) and 2,3-naphthalenediol, 3-hydroxy-2-naphthoic acid (b). The spectrum of neat titanium dioxide nanoparticles is shown as a reference. Spectra recorded for aqueous colloidal solutions at pH = ~2, c_{TiO₂} = 4 g dm⁻³, particle diameter = 3–10 nm, [ligand] = 10⁻⁴ mol dm⁻³.**Table 5**Energies (eV) of lowest singlet excited states with dominating HOMO → LUMO character for various [TiL(OH)₂] model complexes as calculated using TD-DFT method on the B3PW91/DGDZVP level of theory.

Ligand	R ₁ = OH R ₂ = OH	R ₁ = OH R ₂ = COOH	R ₁ = COOH R ₂ = COOH
			
	3.30	3.27	3.71
	2.46	3.11	3.79
	2.34	2.77	3.12
	1.83	2.39	2.66

semiconductor systems, as well as efficiency of photosensitization and reactivity of the excited state.

Modeling performed for a simple [(H₂O)Fe(CN)₄–C≡N–Ti(OH)₃]^{2–} (L = H₂O, NH₃, aliphatic thioether) model systems enabled recognition of the characters of HOMO and LUMO. The HOMO orbital of this species is localized mainly on equatorial cyanide ligands and the iron ion, while the LUMO on bridging cyanide ligand and on titanium(IV) ion [55]. This facilitates an efficient photoinduced electron transfer between Ti^{IV} and Fe^{II} centers. The low energy transition (HOMO → LUMO) in this complex includes electron transfer from the cyanoferrate moiety towards the titanium center with formation of Ti^{III} and Fe^{III}. Similar results were reported for [Fe(CN)₆]^{4–} bound to the TiO₂ nanocluster [54].

4. Photoreactivity of titanium(IV) surface complexes

4.1. Photoelectrochemistry

Surface titanium(IV) complexes may drastically accelerate interfacial electron transfer from the conduction band of titanium

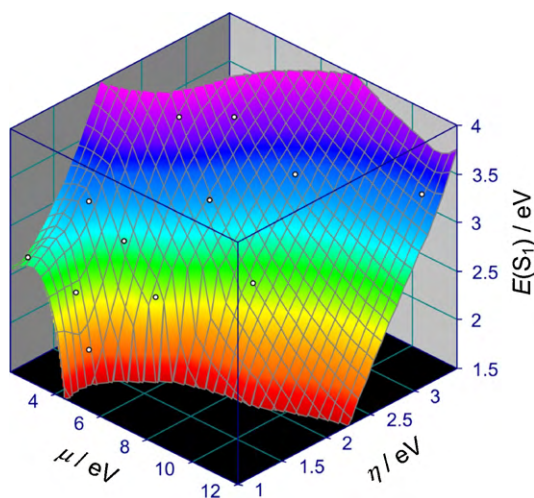


Fig. 12. Correlation between Mulliken electronegativity (μ), global hardness (η) of the ligand and the energy of the lowest LMCT transition ($E(S_1)$) in the model complexes $[\text{TiL}(\text{OH})_2]$ as calculated using TD-DFT method on the B3PW91/DGDZVP level of theory.

dioxide to electron acceptors in solution (e.g. methylviologen, oxygen) [101,40]. Modification with phthalates and salicylates gives much more pronounced effects compared to modification with aromatic monocarboxylic acids (e.g. benzoic acid) [101]. Also photocurrent measurements made for electrodes covered by such materials confirm an efficient photosensitization and interfacial electron transfer (Fig. 13). Irradiation with ultraviolet light induces anodic photocurrents in the case of working electrodes covered with either neat or modified titanium dioxide. Remarkable non-zero values of photocurrents were recorded upon visible light excitation (400 to 550–650 nm) only in the case of ITO-electrodes covered with modified TiO_2 pointing at efficient photosensitization effect.

Photoelectrochemical properties of titanium dioxide sensitized by dinuclear $[\text{L}_n\text{Fe-CN-TiL}_n]$ complexes are particularly interesting. This group of materials, involving hexacyanoferrate and pentacyanoferrate moieties, shows the PEPS effect (photoelectrochemical photocurrent switching) [55,56,85,102–105]. The direction of generated photocurrent depends on the applied potential and therefore on the oxidation state of the surface iron species, on wavelength of incident light and composition of the electrolyte. The dependence of photocurrent on potential applied to the ITO-electrode covered with TiO_2 modified with hexa-

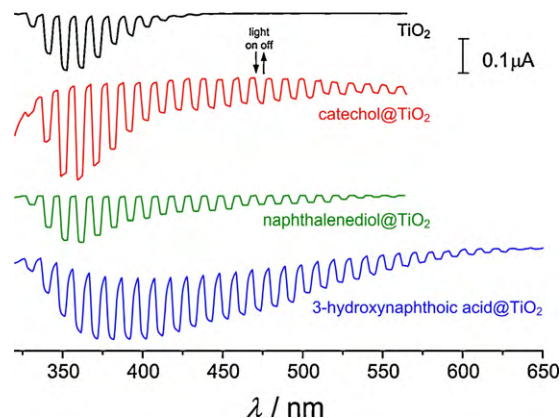


Fig. 13. Dependence of photocurrent generated at ITO-working electrodes covered with TiO_2 nanoparticles (black line) and nanoparticles with chemisorbed catechol (red), naphthalenediol (green) and 3-hydroxynaphthoic acid (blue) on wavelength of incident light. Arrows indicate opening of the shutter. The measurements were performed in a three-electrode set-up with platinum and silver/silver chloride electrodes as auxiliary and reference electrodes, respectively, at potential 0.5 V vs. Ag/AgCl in 0.1 mol dm^{-3} KNO_3 aqueous solution.

cyanoferrate ($[\text{Fe}(\text{CN})_6]^{4-}@\text{TiO}_2$) upon chopped light is shown in Fig. 14a. At potentials higher than the redox potential of the $[\text{Fe}(\text{CN})_6]^{3-}/[\text{Fe}(\text{CN})_6]^{4-}$ couple the anodic photocurrents characteristic for unmodified TiO_2 are observed. Anodic photocurrents result from the electron transfer from the conduction band to the electrode with concomitant electrolyte oxidation by holes from the valence band. The excitation of the oxidized surface species does not take place, also photosensitization is not achieved. Under such conditions only excitation of the semiconductor matrix with ultraviolet light may result in photocurrent generation (anodic).

At lower potentials the photocurrents switch to cathodic (Fig. 14a). The switching potential at which the photocurrent direction changes correlates very well with redox potential of the iron moiety. Only the reduced form of iron (Fe^{II}) can contribute to cathodic photocurrent generation. Excitation of the reduced surface species generates an electron in the conduction band as a result of $\text{Fe}^{\text{II}} \rightarrow \text{Ti}^{\text{IV}}$ charge transfer. Due to a significant negative polarization of the electrode the electron transfer from the conduction band to the electrode is not favored, but the reverse process, i.e. reduction of the electron acceptor in the electrolyte and a concomitant electron transfer from the electrode to the photochemically oxidized surface moiety (Fe^{III}), takes place. The cathodic photocurrent appears and surface complex is regenerated (Fe^{II} , Ti^{IV}). In the

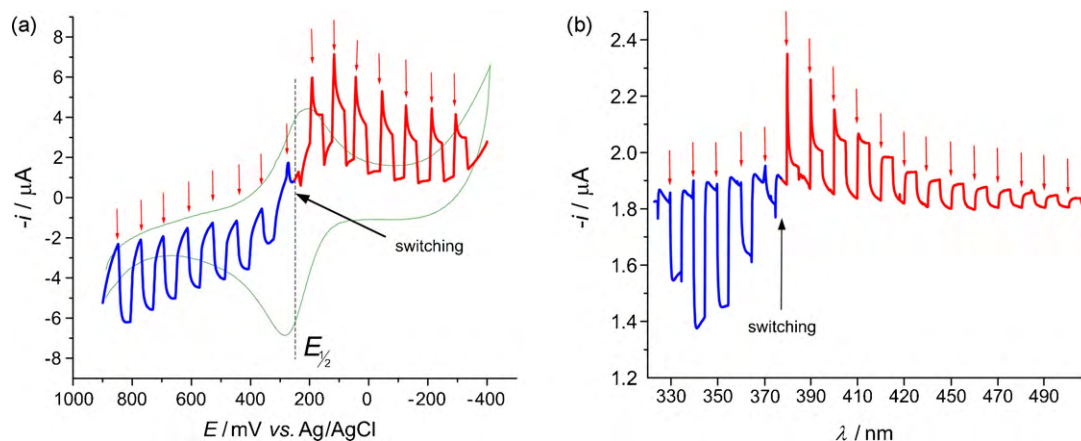


Fig. 14. Dependence of photocurrent generated at ITO-working electrode covered with $[\text{Fe}(\text{CN})_6]^{4-}@\text{TiO}_2$ on applied potential (a: $\lambda = 350$ nm, scan rate 10 mV s^{-1}) and excitation wavelength (b: $E = 200$ V vs. Ag/AgCl). Anodic photocurrents are shown in blue, cathodic—in red. For comparison the cyclic voltammogram recorded in the dark for the $[\text{Fe}(\text{CN})_6]^{4-}@\text{TiO}_2$ electrode is shown in (a). Arrows indicate opening of the shutter. Adapted from Ref. [102].

case of air-equilibrated systems oxygen molecule plays the role of the electron acceptor ($E_{\text{O}_2/\text{O}_2^-} = -0.16 \text{ V vs. NHE}$) [106,107]. Direct excitation of the semiconductor also results in cathodic photocurrents.

At certain range of potentials, close to the redox potential of the $[\text{Fe}(\text{CN})_6]^{3-}/[\text{Fe}(\text{CN})_6]^{4-}$ couple, the photocurrent may change between anodic (direct excitation of the semiconductor, UV light) and cathodic (MBCT, visible light), Fig. 14b. Described effect of the photocurrent switching upon change of either the electrode potential or colour of incident light is called the PEPS effect.

4.2. Photocatalysis

Photocatalytic processes induced at the surface of TiO_2 modified with Ti^{IV} complexes are determined by two main factors: the effect of photosensitization and good chemisorption of organic molecules being at the same time ligands and targets for photo-generated reactive oxygen species. Although photosensitization of titanium dioxide by surface titanium(IV) complexes may be very efficient (*vide supra*) in the presence of oxygen photostability of surface complexes is very limited.

The presence of electrons in conduction band of TiO_2 enables generation of reactive oxygen species (ROS) as a consequence of adsorbed oxygen reduction [6,108]. Superoxide anions, hydrogen peroxide and hydroxyl radicals are responsible for oxidation of majority of organic species accessible at the photocatalyst surface or in its vicinity. Also organic ligands may be a target of ROS attack. Therefore surface complexes of titanium(IV) are not photostable in the presence of oxygen. On the other hand complexation of organic pollutants at the photocatalyst surface facilitates their efficient oxidation [15,19,109,110]. Use of titanium(IV) complexes with organic ligands as photosensitizers may be considered only in the cases when long term activity is not required (compare *Potential applications and perspectives*).

Despite a generally low photostability of surface complexes there are some reports on a relatively good photostability of some ligands chemisorbed at TiO_2 . The long-time photostability tests of dopamine-modified TiO_2 colloids (dopamine can be considered as a catechol derivative) have shown that this material can resist exposure to laser pulses (450 nm) and daylight for several years [111]. This unusual stability of the surface complex with dopamine is related to the bidentate binding of dopamine [39]. Irreversible oxidation of free dopamine occurs exclusively upon formation of radicals localized at hydroxyl groups of this enediol molecule. In the case of the bound dopamine molecule with both hydroxyl groups coordinated to surface titanium, oxidation is reversible and proceeds via formation of carbon-centered radicals of the dopamine aromatic ring. Upon illumination of the system photogenerated holes localized at carbon-centered radicals recombine with electrons from the conduction band of TiO_2 particles preventing irreversible degradation of dopamine.

An interesting application of photocatalytic processes at dopamine-modified TiO_2 was proposed by Rajh and co-workers [111]. DNA oligonucleotides covalently linked to dopamine-modified nanoparticles of TiO_2 were used to establish an efficient light-induced crosstalk across the biomolecule and metal oxide surface—light-induced extended charge separation in these systems was useful as a fingerprint of DNA hybridization and DNA sequence. The efficiency of photocatalytic silver deposition at this system depends on the compatibility of single stranded DNAs. The amount of deposited metallic silver was sensitive to the presence of a single mismatch of nucleic base pairs in DNA sequence. Understanding electron tunneling in such systems provides a platform for investigation of biorelevant redox reactions as a function of biomolecule conformation.

5. Potential applications and perspectives

Spectral and photocatalytic properties of titanium dioxide modified with organic compounds or cyanometallate anions to yield various titanium(IV) surface complexes may constitute a good platform for various applications, from medicine to optoelectronics [6,7,112]. Photocatalysis based on reactive oxygen species generation upon visible light irradiation may assure detoxification and disinfection of various environments. Considering such applications the limited stability of described systems should be taken into account. Therefore titanium dioxide sensitized with organic ligands may be applied for disinfection of disposable equipment, as a component of photosterilizing sprays, etc. Studies on antimicrobial properties of such materials may lead to the development of photodrugs used for instance for curing inflammations, wound disinfection, etc. In such applications photodynamic inactivation (PDI) of microorganisms requires rather high photoactivity and non-toxicity of active materials than their long (photo)stability.

The possibility of attaching a wide variety of biomolecules to TiO_2 nanoparticles without the loss of photocatalytic activity enables their use in biological and biomedical applications. Adaptation (or incorporation) of nanostructured materials into biomedical devices and systems has been of great interest in recent years [113,114]. Through the modification of existing nano-scale materials it is possible to control and enhance the properties of such materials in a desired way, and impart them with biological properties and functionalities for better integration with biological systems. These modified nanostructured materials can bring new and unique capabilities to a variety of biomedical applications ranging from implant engineering and modulated drug delivery, to clinical biosensors and diagnostics. Growing number of reports on development of nanostructured materials for biomedical applications shows their great potential. The methods and technologies used to modify nanostructured materials use various techniques and protocols depending on the surface physicochemistry of material to be modified.

Modification of nanomaterials with biomolecules is often indispensable to reach biocompatibility and functionality of nanoparticles. Chemically or physically surface-bound biospecific molecules offer sites for immobilization of other ligands specific to these molecules. TiO_2 surface offers vast possibilities of surface modification by compounds capable of coordination to Ti^{IV} . Immobilization of specific ligands can be achieved through biologically specific reactions, such as antibody–antigen [115], receptor–ligand [116], avidin–(or streptavidin)–biotin [117], and DNA–DNA hybridization [118]. For instance, titanium dioxide nanoparticles modified with folic acid [116] may be selectively accumulated at the surface of human cancer cells as a result of binding by folate receptors, often overexpressed at the surface of this type of cells [119]. As a consequence the nanoparticles are internalized [116]. This specific recognition of cancer cells by surface-modified TiO_2 nanoparticles together with the photosensitization effect and photocatalytic activity might constitute a prospective approach to photodynamic therapy (PDT).

One of the major problem with inorganic/hybrid nanomaterials is their stability under physiological conditions (blood/plasma environment). Poly(ethylene glycol) (PEG) is a common biocompatible compound used to overcome this problem. PEG anchored to the surface of nanoparticles effectively prevents particle agglomeration and protein adsorption thus enabling extended activity of nanoparticles in biological systems. This surface-exposed hydrophilic coating of PEGylated nanoparticles reduces natural blood opsonization and increases circulation time, which is critical for drug delivery carriers [120]. Furthermore, in order to introduce reactive groups for immobilization of other ligand molecules, heterobifunctional PEGs have been used for modification of nanoparticles [121].

Considering the cytotoxicity and biocompatibility of the surface-modified materials various factors have to be taken into account and the complexity of the issue rises. In addition to verification of cytotoxicity of a hybrid nanomaterial also its constituents, *i.e.* core material and modifiers alone cannot be toxic, since possible degradation of the material can occur under physiological conditions in the presence of various factors (*e.g.* presence of enzymes, various types of cells and compartment-dependent microenvironment). Surface chemistry of metals oxides in aspect of biological and biochemical studies is a very vast and complex area [122]. Moreover, properties of nanostructured materials may differ substantially from those observed for bulk materials. Toxicological studies have shown a clear correlation between increased toxicity of some particles with decreasing particle size. Although nanoparticles are not always more toxic than microparticles, a high toxicity of nano-CuO has been proven [123]. Karlsson et al. report low toxicity of iron oxides particles independently on their size, similarly TiO₂ particles have been claimed to be non-cytotoxic [123]. Other authors report a low cytotoxicity and little ability to cause mitochondrial damage by TiO₂ nanoparticles [124,125], but recently cytotoxic effects of TiO₂ nanoparticles (21 nm) in BEAS-2B cells was observed [126]. Surprisingly, TiO₂ microparticles caused significantly higher level of DNA damage than corresponding nanoparticles, what is in contrast to most of the *in vitro* and *in vivo* studies on inflammatory potential. It is known however that the various crystal structures of titanium dioxide (*i.e.* anatase or rutile) produce different toxicological responses pointing at higher toxicity of anatase [127]. It is also postulated that *in vivo* toxicity of TiO₂ particles does not depend on surface area and size, but on surface properties of this oxide [128]. Ultrafine TiO₂ particles show ability to be taken up by cells but their potential to penetrate to the nucleus is more questionable [126,129].

Beside medical applications of titanium(IV) surface complexes these materials may find application in optoelectronics. Photoelectrochemical properties of titanium dioxide sensitized by dinuclear L_nFe–CN–TiL_n complexes due to the direct photosensitization constitute a universal platform for construction of various switches, logic gates and more complex devices, including programmable logic gates. Up to date most of the molecular scale logic devices operated in solutions and used various “chemical” inputs, whereas the PEPs-based optoelectronic devices use exclusively electric and optical signals. These purely inorganic materials are also much more stable as compared to those with organic ligands and therefore their operation may not be significantly limited.

As demonstrated in this paper the direct photosensitization of titanium dioxide by surface titanium(IV) complexes is not only an issue of basic research. Simplicity of formation of such complexes together with high efficiency of photoinduced electron transfer processes may facilitate various practical applications of these systems.

Acknowledgements

This work was supported by Polish Ministry of Science and Higher Education (grant nos. 1609/B/H03/2009/36 and DWM/N112/COST/2008). All the DFT calculations were performed at Academic Computer Centre CYFRONET AGH within computational grant MEiN/SGI3700/UJ/085/2006.

References

- [1] J.G. Vos, R.J. Forster, T.A. Keyes, *Interfacial Supramolecular Assemblies*, John Wiley & Sons Ltd., Chichester, 2003.
- [2] C. Ashkenasy, D. Cahen, R. Cohen, A. Shanzer, A. Vilan, *Acc. Chem. Res.* 35 (2002) 121.
- [3] A. Vilan, D. Cahen, *Trends Biotechnol.* 20 (2002) 22.
- [4] J.E. Moser, P. Bonnôte, M. Grätzel, *Coord. Chem. Rev.* 171 (1998) 245.
- [5] A. Hagfeldt, M. Grätzel, *Acc. Chem. Res.* 33 (2000) 269.
- [6] K. Szaciłowski, W. Macyk, A. Drzewiecka-Matuszek, M. Brindell, G. Stochel, *Chem. Rev.* 105 (2005) 2647.
- [7] G. Stochel, M. Brindell, W. Macyk, Z. Stasicka, K. Szaciłowski, *Bioinorganic Photochemistry*, Wiley, Chichester, 2009.
- [8] P. Persson, R. Bergström, S. Lunell, *J. Phys. Chem. B* 104 (2000) 10348.
- [9] A. Vittadini, A. Selloni, F.P. Rotzinger, M. Grätzel, *J. Phys. Chem. B* 104 (2000) 1300.
- [10] P.C. Redfern, P. Zapol, L.A. Curtiss, T. Rajh, M.C. Thurnauer, *J. Phys. Chem. B* 107 (2003) 11419.
- [11] U. Diebold, *Surf. Sci. Rep.* 48 (2003) 53.
- [12] P.R. McGill, H. Idriss, *Surf. Sci.* 602 (2008) 3688.
- [13] S.-C. Li, J.-G. Wang, P. Jacobson, X.-Q. Gong, A. Selloni, U. Diebold, *J. Am. Chem. Soc.* 131 (2009) 980.
- [14] H.A. Al-Abadleh, V.H. Grassian, *Surf. Sci. Rep.* 52 (2003) 63.
- [15] S. Tunesi, M. Anderson, *J. Phys. Chem.* 95 (1991) 3399.
- [16] R. Rodriguez, M.A. Blesa, A.E. Regazzoni, *J. Colloid Interface Sci.* 177 (1996) 122.
- [17] A.D. Weisz, A.E. Regazzoni, M.A. Blesa, *Solid State Ionics* 143 (2001) 125.
- [18] Y. Liu, J.I. Dadap, D. Zimdars, K.B. Eiseenthal, *J. Phys. Chem. B* 103 (1999) 2480.
- [19] A.E. Regazzoni, P. Mandelbaum, M. Matsuyoshi, S. Schiller, S.A. Biles, M.A. Blesa, *Langmuir* 14 (1998) 868.
- [20] A. Fahmi, C. Minot, P. Fourre, P. Nortier, *Surf. Sci.* 343 (1995) 261.
- [21] S.J. Hug, D. Bahnemann, *J. Electron. Spectrosc.* 150 (2006) 208.
- [22] K.S. Kim, M.A. Barteau, W.E. Farneth, *Langmuir* 4 (1988) 533.
- [23] V.S. Lusvardi, M.A. Barteau, W.E. Farneth, *J. Catal.* 153 (1995) 41.
- [24] S. Pilikenton, S.-J. Hwang, D. Raftery, *J. Phys. Chem. B* 103 (1999) 11152.
- [25] S.-J. Hwang, D. Raftery, *Catal. Today* 49 (1999) 353.
- [26] W. Xu, D. Raftery, *J. Phys. Chem. B* 105 (2001) 4343.
- [27] L. Gamble, L.S. Jung, C.T. Campbell, *Surf. Sci.* 348 (1996) 1.
- [28] H. Al-Ekabi, N. Serpon, E. Pelizzetti, C. Minero, M.A. Fox, R.B. Draper, *Langmuir* 5 (1989) 250.
- [29] D. Robert, S. Parra, C. Pulgarin, A. Krzton, J.V. Weber, *Appl. Surf. Sci.* 167 (2000) 51.
- [30] J. Arana, E.P. Melian, V.M.R. Lopez, A.P. Alonso, J.M.D. Rodriguez, O.G. Diaz, J.P. Pena, *J. Hazard. Mater.* 146 (2007) 520.
- [31] T.A. Konovalova, L.D. Kispert, V.V. Konovalov, *J. Phys. Chem. B* 103 (1999).
- [32] L. Ojamäe, A. Christian, P. Henrik, P.-O. Käll, *J. Colloid Interface Sci.* 296 (2006) 71.
- [33] S.J. Hug, B. Sulzberger, *Langmuir* 10 (1994) 3587.
- [34] A.D. Weisz, L. Garcia Rodenas, P.J. Morando, A.E. Regazzoni, M.A. Blesa, *Catal. Today* 76 (2002) 103.
- [35] C.B. Mendive, D.W. Bahnemann, M.A. Blesa, *Catal. Today* 101 (2005) 237.
- [36] F.P. Rotzinger, J.M. Kesselman-Truttmann, J.S. Hug, B. Sulzberger, V. Shklover, M. Grätzel, *J. Phys. Chem. B* 108 (2004) 5004.
- [37] P.Z. Araujo, C.B. Mendive, L.A. Garcia Rodenas, P.J. Morando, A.E. Regazzoni, M.A. Blesa, D. Bahnemann, *Colloids Surf. A: Physicochem. Eng. Aspects* 265 (2005) 73.
- [38] T. Rajh, J.M. Nedeljkovic, L.X. Chen, O. Poluektov, M.C. Thurnauer, *J. Phys. Chem. B* 103 (1999) 3515.
- [39] T. Rajh, L.X. Chen, K. Lukas, T. Liu, M.C. Thurnauer, D.M. Tiede, *J. Phys. Chem. B* 106 (2002) 10543.
- [40] J. Moser, S. Punchedewa, P.P. Infelta, M. Grätzel, *Langmuir* 7 (1991) 3012.
- [41] P.Z. Araujo, P.J. Morando, M.A. Blesa, *Langmuir* 21 (2005) 3470.
- [42] T. Tachikawa, Y. Takai, S. Tojo, M. Fujitsuka, T. Majima, *Langmuir* 22 (2006) 893.
- [43] P.A. Connor, K.D. Dobson, A.J. McQuillan, *Langmuir* 11 (1995) 4193.
- [44] S. Tunesi, M. Anderson, *Langmuir* 8 (1992) 487.
- [45] Q. Guo, I. Cocks, E.M. Williams, *Surf. Sci.* 393 (1997) 1.
- [46] F. Gajardo, A.M. Leiva, B. Loeb, A. Delgadillo, J.R. Stromberg, G.J. Meyer, *Inorg. Chim. Acta* 361 (2008) 613.
- [47] D. Kuciauskas, M.S. Freund, H.B. Gray, J.R. Winkler, N.S. Lewis, *J. Phys. Chem. B* 105 (2001) 392.
- [48] A. Islam, H. Sugihara, K. Hara, L.P. Singh, R. Katoh, M. Yanagida, Y. Takahashi, S. Murata, H. Arakawa, *Inorg. Chem.* 40 (2001) 5371.
- [49] G. Sauve, M.E. Cass, S.J. Doig, I. Laueremann, K. Pomykal, N.S. Lewis, *J. Phys. Chem. B* 104 (2000) 3488.
- [50] H. Kisch, G. Burgeth, W. Macyk, *Adv. Inorg. Chem.* 56 (2004) 241.
- [51] G. Burgeth, H. Kisch, *Coord. Chem. Rev.* 230 (2002) 40.
- [52] W. Macyk, H. Kisch, *Chem. Eur. J.* 7 (2001) 1862.
- [53] W. Macyk, G. Burgeth, H. Kisch, *Photochem. Photobiol. Sci.* 2 (2003) 322.
- [54] F. De Angelis, A. Tilotta, A. Selloni, *J. Am. Chem. Soc.* 126 (2004) 15024.
- [55] M. Hebda, G. Stochel, K. Szaciłowski, W. Macyk, *J. Phys. Chem. B* 110 (2006) 15275.
- [56] K. Szaciłowski, W. Macyk, M. Hebda, G. Stochel, *Chem. Phys. Chem.* 7 (2006) 2384.
- [57] M. Yang, D.W. Thompson, G.J. Meyer, *Inorg. Chem.* 41 (2002) 1254.
- [58] H. Sato, K. Ono, T. Sasaki, A. Yamagishi, *J. Phys. Chem. B* 107 (2003) 9824.
- [59] X. Chen, S.S. Mao, *Chem. Rev.* 107 (2007) 2891.
- [60] J.I. Pankove, *Optical Processes in Semiconductors*, Dover Publications, Inc., Mineola, NY, 1975.
- [61] N.A. Anderson, T. Lian, *Annu. Rev. Phys. Chem.* 56 (2005) 491.
- [62] M.K. Bruska, K. Szaciłowski, J. Piechota, *Mol. Simulat.* 35 (2009) 567.
- [63] S. Braun, W.R. Salaneck, M. Fahlman, *Adv. Mater.* 21 (2009) 1450.
- [64] R.L. McCreery, *Chem. Mater.* 16 (2004) 4477.

- [65] D.S. Seferos, S.A. Trammell, G.C. Bazan, J.G. Kushmerick, *Proc. Natl. Acad. Sci.* 102 (2005) 8821.
- [66] F. Anariba, R.L. McCreery, *J. Phys. Chem. B* 106 (2002) 10355.
- [67] M. Galperin, A. Nitzan, *Phys. Rev. Lett.* 95 (2005) 206802.
- [68] M. Galperin, A. Nitzan, *J. Chem. Phys.* 124 (2006) 234709.
- [69] M. Galperin, A. Nitzan, M.A. Ratner, *Phys. Rev. Lett.* 96 (2006) 166803.
- [70] A. Nitzan, *Annu. Rev. Phys. Chem.* 52 (2001) 681.
- [71] C. Creutz, B.S. Brunschwig, N. Sutin, *J. Phys. Chem. B* 109 (2005) 10251.
- [72] C. Creutz, B.S. Brunschwig, N. Sutin, *J. Phys. Chem. B* 110 (2006) 25181.
- [73] C. Creutz, B.S. Brunschwig, N. Sutin, *Chem. Phys.* 324 (2006) 244.
- [74] D.M. Adams, L. Brus, C.E.D. Chidsey, S. Creager, C. Creutz, C.R. Kagan, P.V. Kamat, M. Lieberman, S. Lindsay, R.A. Marcus, R.M. Metzger, M.E. Michel-Beyerle, J.R. Miller, M.D. Newton, D.R. Rolison, O. Sankey, K.S. Schanze, J. Yardley, X. Zhu, *J. Phys. Chem. B* 107 (2003) 6668.
- [75] T. Sakata, K. Hashimoto, M. Hiramoto, *J. Phys. Chem.* 94 (1990) 3040.
- [76] O. Kitao, *J. Phys. Chem. C* 111 (2007) 15889.
- [77] M.V. Lebedev, *Progr. Surf. Sci.* 70 (2002) 153.
- [78] D.M. Newns, *Phys. Rev.* 178 (1969) 1123.
- [79] C.D. Lindstrom, X.-Y. Zhu, *Chem. Rev.* 106 (2006) 4281.
- [80] E. Vrachnou, M. Grätzel, A.J. McEvoy, *J. Electroanal. Chem.* 258 (1989) 193.
- [81] E. Vrachnou, N. Vlachopoulos, M. Grätzel, *J. Chem. Soc. Chem. Commun.* (1987) 868.
- [82] H.N. Gosh, J.B. Ashbury, Y. Weng, T. Lian, *J. Phys. Chem. B* 102 (1998) 10208.
- [83] M. Khoudiakov, A.R. Parise, B.S. Brunschwig, *J. Am. Chem. Soc.* 125 (2003) 4637.
- [84] W. Macyk, G. Stochel, K. Szaciłowski, *Chem. Eur. J.* 13 (2007) 5676.
- [85] J.A. Harris, K. Trotter, B.S. Brunschwig, *J. Phys. Chem. B* 111 (2007) 6695.
- [86] C. Creutz, M.H. Chou, *Inorg. Chem.* 47 (2008) 3509.
- [87] L.G.C. Rego, V.S. Batista, *J. Am. Chem. Soc.* 125 (2003) 7989.
- [88] I.A. Janković, Z.V. Šaponjić, M.I. Čomor, J.M. Nedelković, *J. Phys. Chem. C* 113 (2009) 12645.
- [89] Y. Xu, W.-K. Chen, S.-H. Liu, M.-J. Cao, J.-Q. Li, *Chem. Phys.* 331 (2007) 275.
- [90] M. Vega-Arroyo, P.R. LeBreton, T. Rajh, P. Zapol, L.A. Curtiss, *Chem. Phys. Lett.* 406 (2005) 306.
- [91] N.J. Cherepy, G.P. Smestad, M. Grätzel, J.Z. Zhang, *J. Phys. Chem. B* 101 (1997) 9342.
- [92] K. Szaciłowski, W. Macyk, G. Stochel, *J. Mater. Chem.* 16 (2006) 4603.
- [93] S. Gawęda, G. Stochel, K. Szaciłowski, *J. Phys. Chem. C* 112 (2008) 19131.
- [94] T. Koopmans, *Physica* 1 (1934) 104.
- [95] J.F. Janak, *Phys. Rev. B* 18 (1978) 7165.
- [96] M.L. Knotek, P.J. Feibelman, *Phys. Rev. Lett.* 40 (1978) 964.
- [97] R. Asahi, Y. Haga, W. Mannstadt, A.J. Freeman, *Phys. Rev. B* 61 (2000) 7459.
- [98] S.I. Gorelsky, AOMix: Program for Molecular Orbital Analysis, University of Ottawa, 2007, <http://www.sg-chem.net>.
- [99] S. Gawęda, G. Stochel, K. Szaciłowski, *Chem. Asian J.* 2 (2007) 580.
- [100] K.A. Walters, D.A. Gaal, J.T. Hupp, *J. Phys. Chem. B* 106 (2002) 5139.
- [101] A. Hagfeldt, M. Grätzel, *Chem. Rev.* 95 (1995) 49.
- [102] K. Szaciłowski, W. Macyk, *Comp. Rend. Chim.* 9 (2006) 315.
- [103] K. Szaciłowski, W. Macyk, *Solid-State Electron.* 50 (2006) 1649.
- [104] K. Szaciłowski, W. Macyk, *Chimia* 61 (2007) 831.
- [105] K. Szaciłowski, W. Macyk, G. Stochel, *J. Am. Chem. Soc.* 128 (2006) 4550.
- [106] D.T. Sawyer, J.S. Valentine, *Acc. Chem. Res.* 14 (1981) 393.
- [107] D.M. Stanbury, *Adv. Inorg. Chem.* 33 (1989) 69.
- [108] W. Macyk, A. Franke, G. Stochel, *Coord. Chem. Rev.* 249 (2005) 2437.
- [109] V. Subramanian, V.G. Pangarkar, A.A.C.M. Beenackers, *Clean Prod. Process.* 2 (2000) 149.
- [110] D. Vione, C. Minero, V. Maurino, M.E. Carloti, T. Picatotto, E. Pelizzetti, *Appl. Catal. B: Environ.* 58 (2005) 79.
- [111] J. Liu, L. de la Garza, L. Zhang, N.M. Dimitrijevic, X. Zuo, D.M. Tiede, T. Rajh, *Chem. Phys.* 339 (2007) 154.
- [112] K. Szaciłowski, *Chem. Rev.* 108 (2008) 3481.
- [113] C.M. Niemeyer, *Angew. Chem. Int. Ed. Engl.* 40 (2001) 4128.
- [114] E. Katz, I. Willner, *Angew. Chem. Int. Ed.* 43 (2004) 6042.
- [115] C.X. Zhang, Y. Zhang, X. Wang, Z.M. Tang, Z.H. Lu, *Anal. Biochem.* 320 (2003) 136.
- [116] M.O. Oyewumi, R.J. Mumper, *Int. J. Pharm.* 251 (2003) 85.
- [117] S.V. Vinogradov, T.K. Bronich, A.V. Kabanov, *Adv. Drug Deliv. Rev.* 54 (2002) 135.
- [118] M.J. Moghaddam, S. Taylor, M. Gao, S.M. Huang, L.M. Dai, M.J. McCall, *Nano Lett.* 4 (2004) 89.
- [119] S. Wang, P.S. Low, *J. Control. Release* 53 (1998) 39.
- [120] P. Calvo, B. Gouritin, H. Villarroja, F. Eclancher, C. Giannavola, C. Klein, J.P. Andreux, P. Couvreur, *Eur. J. Neurosci.* 15 (2002) 1317.
- [121] N. Kohler, G.E. Fryxell, M.Q. Zhang, *J. Am. Chem. Soc.* 126 (2004) 7206.
- [122] G.E. Brown Jr., V.E. Henrich, W.H. Casey, D.L. Clark, C. Eggleston, A. Felmy, D.W. Goodman, M. Grätzel, G. Maciel, M.I. McCarthy, K.H. Nealson, D.A. Sverjensky, M.F. Toney, J.M. Zachara, *Chem. Rev.* 99 (1999) 77.
- [123] H.L.L. Karlsson, J. Gustafsson, P. Cronholm, L. Möller, *Toxicol. Lett.* 188 (2009) 112.
- [124] S.M. Hussain, K.L. Hess, J.M. Gearhart, K.T. Geiss, J.J. Schlager, *Toxicol. in Vitro* 19 (2005) 9.
- [125] H.A. Jeng, J. Swanson, *J. Environ. Sci. Health A: Tox. Hazard. Subst. Environ. Eng.* 41 (2006) 2699.
- [126] E.J. Park, J. Yi, K.H. Chung, D.Y. Ryu, J. Choi, K. Park, *Toxicol. Lett.* 180 (2008) 222.
- [127] C.M. Sayes, R. Wahi, P.A. Kurian, Y. Liu, J.L. West, K.D. Ausman, D.B. Warheit, V.L. Colvin, *Toxicol. Sci.* 92 (2006) 174.
- [128] D.B. Warheit, T.R. Webb, C.M. Sayes, V.L. Colvin, K.L. Reed, *Toxicol. Sci.* 91 (2006) 227.
- [129] S. Singh, T. Shi, R. Duffin, C. Albrecht, D. van Berlo, D. Hohn, B. Fubini, G. Martra, I. Fenoglio, P.J. Borm, R.P. Schins, *Toxicol. Appl. Pharmacol.* 222 (2007) 141.